Framework development for robust design of novel aircraft concept

Marco Saporito, Andrea da Ronch, Peter Schmollgruber, Nathalie Bartoli

AerospaceEurope Conference2020
BORDEAUX, FRANCE | 25 - 28 FEBRUARY 2020
HOSTED BY : CEAS 3AF

FRAMEWORK DEVELOPMENT FOR ROBUST DESIGN OF NOVEL AIRCRAFT CONCEPTS

Marco Saporito [(1)], Andrea Da Ronch [(1)], Peter Schmollgruber[(2)], Nathalie Bartoli[(2)]

[(1)] University of Southampton, Southampton, S017 1BJ, United Kingdom.
Email: m.saporito@soton.ac.uk, a.da-ronch@soton.ac.uk

[(2)] ONERA/DTIS, Université de Toulouse, F-31055 Toulouse, France.
Email: Peter.Schmollgruber@onera.fr, Nathalie.Bartoli@onera.fr

KEYWORDS: Aircraft design, Multidisciplinary Analysis and Optimization, Aerodynamics.

ABSTRACT:

One of the challenges in Multidisciplinary Design Analysis and Optimization is raised by the fidelity of the methods and tools used within each single discipline. This element, introducing uncertainty in predictions, is neglected generally. In this work, a framework is built to analyse the impact that the fidelity of the aerodynamic model has on four key figures of merit, including Maximum Take-off Weight, maximum Lift-to-drag ratio, fuel weight and take-off length. It is found that the aircraft configuration with minimum fuel weight computed with two aerodynamic models differs significantly, with large variations in terms of predicted fuel weight and wing planform.

1. INTRODUCTION

As environmental requirements become more and more urgent, reduction of emissions in commercial aviation is targeted with increasing pressure both by research and industrial [1**Erreur ! Source du renvoi introuvable.**, 12, 26]. A large effort is put on the exploration of disruptive technologies and configurations that may lead to a new generation of highly efficient aircraft [2, 3].
Most innovation strategies arise at the three levels of propulsion, structures and aerodynamics. Technologies such as electric/hybrid propulsion and distributed propulsion are receiving large attention [4], as well as cutting-edge structural solutions including composites-rich structures, bio-inspired materials, morphing structures [22], foldable wings [23,24], to just name a few.
From the aerodynamic side, the tendency is to promote efficient layouts such as blended wing-body configurations [5], box-wing configurations [14], and very high aspect ratio wings [6] (see Fig. 1). As usual in aerospace design, the implementation of such choices involves important implications on several disciplines. For instance, high aspect ratio wings accentuate aeroelastic issues and affect stability, control strategies and pilot coupling [7]. Therefore, the exploration of disruptive concepts needs to be accompanied by analysis and optimization frameworks as multidisciplinary as possible, even at conceptual or preliminary design stages [8]. Failing to provide adequate multidisciplinary capabilities early in the design may lead to severe consequences such as expensive corrections later in the process, or even to the failure of the whole process [7]. To report a relevant case, after finding that divergent flutter may occur under certain conditions in the Boeing B747-8 and B747-8F, reparations and software updates had to be applied [9], with costs for the company and the operators and some damage to the company's image.

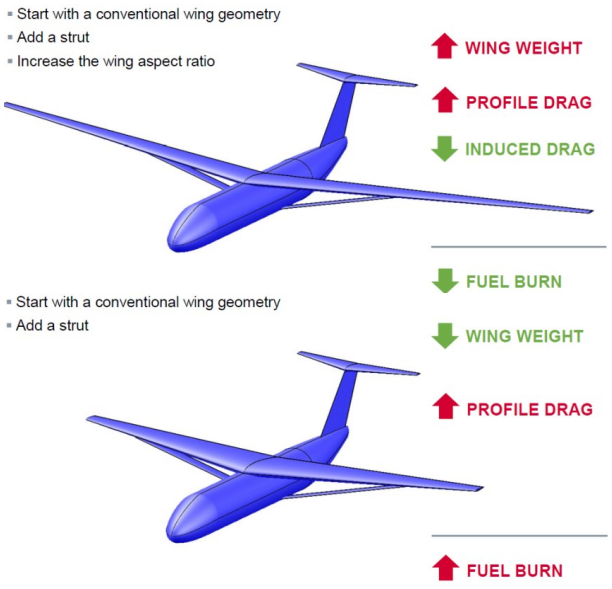

Figure 1: Comparison of conventional and high aspect ratio concepts, from [6]:

The added knowledge arising from a multidisciplinary approach has motivated a large effort in the research and industrial environments towards the implementation of integrated tools for aerospace vehicles design. With the support of

increasingly powerful computers, multidisciplinary analysis and optimization (MDAO) for aircraft design has known significant progress. Together with the numerous achievements, though, several issues still remain challenging and stimulate ongoing efforts in the research community.
For instance, as the aircraft design involves several disciplines, each of which requires different tools and handling a large body of information, the exchange of data between modules represents a crucial question [15]. The definition of common programming languages and data storage formats becomes a key enabler for the effectiveness of the whole framework [16].
Another critical point is the choice of an appropriate model and numerical strategies for each of the involved disciplines. The design team, as well as the single specialist, have at their disposal a broad set of analysis methods of different fidelities. A proper design framework should be implemented in such a way that the appropriate fidelity level is employed for each maturity status of the design process. Often, effort is put on introducing as much physics as possible since the earliest stages by some clever multifidelity approaches. The strategy is to exploit information from a few expensive higher-fidelity analyses to correct and enrich the results of the lower-fidelity tool. This can be done either by directly merging the two solvers in a new hybrid tool [17-19], or by deriving a surrogate model through data sets from multiple tools [20, 21]. The adoption of such strategies and the choice of the appropriate fidelity levels for different design purposes are widely discussed in [13]. When developing an MDAO framework, the assessment of the applicability of all the different analysis tools and their impact in terms of accuracy of the results is a necessary task. In fact, it is desirable to provide the highest possible flexibility towards the exploration of wide design spaces, and all the integrated tools should prove capable to handle large ranges of variables and physical conditions.
The complexity of the MDAO tasks is even increased by the fact that any fidelity level is inherently affected by uncertainties, the most relevant being those related with mass and balance, and aerodynamic performances. Uncertainty quantification and management in MDAO applications is an interesting challenge, at the centre of several research activities [10, 25]. If properly addressed, it would improve the quality of the design outcomes providing key information on the robustness and reliability of the results.
The long term aim of the project here discussed, still ongoing, is to provide robust design capabilities in the context of MDAO for modern aircraft concepts, able to comply with all the discussed requisites, reliable against wide design spaces and robust against the major sources of uncertainty.
The present work focuses on the actual, intermediate state of implementation of such a framework, discussing its capabilities, limits and faced challenges. This is done by employing the framework for design exploration and optimization and comparing the effects of different fidelities of the aerodynamic models. To this purpose, two consecutive objectives were established.
The first objective is to compare the effect of two different aerodynamic models on the overall results of a conceptual multidisciplinary aircraft sizing process. To this end, a set of design candidates was evaluated with both the models and some relevant performance indices were compared. The dispersion of the results was used to assess the robustness of the sizing tool predictions with respect to the perturbation of the most relevant aerodynamic design variables.
The second objective is to perform an optimization study on a baseline configuration and compare the optimal designs obtained for each of the two aerodynamic fidelity levels available within the MDA framework.
The MDA framework and the aerodynamic models are presented in Sections 2 end 3. The adopted methodology is described in Section 4, whereas the selected test case is outlined in Section 5. Results are presented and discussed in Section 6. Finally, conclusions are given in Section 7.

2. AIRCRAFT SIZING TOOL

The adopted aircraft sizing tool, FAST (Fixed-wing Aircraft Sizing Tool) was provided by ONERA and ISAE-SUPAERO. It is conceived as a quick and effective conceptual design tool for traditional tube and wing configurations. The user specifies a series of Top Level Requirements and the framework estimates the required fuel consumption through a series of sizing loops involving modular analyses for the key disciplines, namely flight mechanics, aerodynamics, structures, propulsion, weight and balance. The original approach is based on a point mass approximation together with semi-empirical equations for performance and aerodynamic predictions. This allows high computational efficiency and accuracy to be achieved as long as traditional concepts are treated.
The propulsion module can be based either on a dataset from the CeRAS project [27], or an analytical model that provides thrust and fuel consumption as function of altitude and flight speed [28].
The performance module gathers all the information from the disciplinary modules and performs a time-marching simulation of the full mission.
Sizing and positioning of components are iteratively updated during the design loops through dedicated geometry, weight and balance modules. Overall aircraft design rules from [32] are used to initially locate the main components, such as wing, tail,

landing gear, etc.
Such features suit the purpose of the present study, as the interest here is to investigate the reliability of simplified models against perturbation of some relevant design variables. In fact, it is always desirable in the conceptual stage to provide robust predictions against possible changes later in more advanced phases of the design process. Moreover, the results obtained with the original knowledge-based code architecture are used in this work in comparison with those from an extended version enabling a more physics-based estimation of the aerodynamic performances.
The framework is fully implemented in Python and all the modules are consistently interfaced through a class hierarchy, whereas all the inputs/outputs are standardized in XML or CPACS [29] format. Such well-structured organization is a key feature to properly manage multidisciplinary frameworks, and it allows modules and models to be updated, extended and switched, and, in turn, the interface within the research community is also facilitated.
With this philosophy, the aerodynamic module was upgraded with an additional model based on the Vortex Lattice Method (VLM) that provides a more flexible, physics-based alternative to the original semi-empirical formulation.
As the focus of this work is mainly on the impact of the aerodynamic model on the overall design outcomes, the following section is dedicated to the description of the two aerodynamic models embedded in FAST. Further details about the framework can be found in [30].

3. AERODYNAMIC MODELS

The purpose of the aerodynamic module is to compute the drag polar, $C_D = f(C_L)$, for different flight conditions. The total drag coefficient is given by three contributions arising from viscous drag, C_{D0}, compressibility, C_{Dc}, induced drag, C_{Di}, and trim drag, C_{Dtrim}. The total drag build-up is obtained as in Eq. 1 [32].

$$C_D = k_{C_D}\left(k_{C_{D0}}C_{D0} + k_{C_{Dc}}C_{Dc} + k_{C_{Di}}C_{Di} + k_{C_{D_{trim}}}C_{D_{trim}}\right) \quad (1)$$

where the coefficients k_i, when available, account for additional corrections due to particular technologies such as winglets.
The viscous drag is obtained by summing and normalizing the friction contributions of all the wetted areas as in Eq. 2, with the friction coefficients given by the Prandtl-Schlichting correlation [33] as in Eq. 3.

$$C_{D0} = \sum_i c_{fi}\, k_{fi}\, \frac{S_{wet,i}}{S_i} \quad (2)$$

$$c_f = \frac{0.455}{(1+0.126M^2)\left(log_{10}(R\ \ e)\right)^{2.58}} \quad (3)$$

The compressibility term is estimated by a semi-empirical formula taking as inputs only Mach number and lift coefficient [32]. Although its validity is not general, the correction is considered acceptable as far as the Mach number does not exceed 0.8 [38].
The remaining two contributions, namely induced and trim drag, are evaluated in this study with two different approaches.
The first one still employs simple analytical functions and semi-empirical corrections. The induced drag is given by Eq. 4 [35], and the Oswald factor e is estimated as in [36]. The contribution due to trim is computed by Eq. 5 as indicated in [32].

$$C_{Di} = \frac{c_L^2}{\pi ARe} \quad (4)$$

$$C_{D\,trim} = 5.89 \times 10^{-4}\, CL \quad (5)$$

The second approach aims at introducing more physics in the aerodynamic predictions, and makes use of an in-house developed VLM solver, which is discussed in the next section. Following the categorization given in [13], the first approach will be hereinafter referred to as level zero (L0), whereas the latter as level one (L1).
Finally, as the wing cross-section is fixed since the beginning of each analysis, and its two-dimensional characteristics are known, the maximum lift coefficient is estimated both for L0 and L1 by Eq. 6 [34, 37].

$$C_{Lmax} = k_w\, C_{lmax}\, cos\Lambda_{25} \quad (6)$$

3.1. Vortex Lattice Method

This method is based on a simplified form of the fluid dynamic equations, which allow efficient three-dimensional computations to be performed with fairly accurate prediction in most subsonic flight conditions, making the method particularly suitable for conceptual design purposes. The assumptions are of inviscid, incompressible and irrotational flow. Under these hypotheses, valid with good approximation in the whole flow field except within the boundary layer, it can be demonstrated [39] that the continuity equation reduces to the Laplace's equation (Eq. 7), where the only boundary condition is that the normal flow component must be zero at the solid boundary (Eq. 8). Here Φ is the velocity potential, n is the normal to the local solid surface and the subscripts $(\ \ )_b$ and $(\ \ )_\infty$ denote the body and the undisturbed flowfield, respectively.

$$\nabla^2\Phi = 0 \quad (7)$$

$$\nabla^2(\Phi_b - \Phi_\infty)\cdot \boldsymbol{n} = 0 \quad (8)$$

The basic idea behind the method is to obtain the solution to the Laplace's equation (Eq. 7) by a distribution of elementary solutions on the problem boundaries (body surface and wake). In fact, because of the principle of superposition, if each elementary function is solution of the Laplace's equation, their linear combination will also be a solution for that equation. Among the several suitable functions, the VLM is based on vortex segments following the Biot-Savart law. The method covers the solid surface with a lattice of vortices whose circulations are initially unknown, and will be determined after enforcing the boundary condition (Eq. 8) in some discrete locations, named collocation points. Once the circulations are known, the aerodynamic force can be computed by means of the Kutta-Jukowsky theorem: $\boldsymbol{F} = \rho V_\infty \times \boldsymbol{\Gamma}$, where $\boldsymbol{F}$ is the aerodynamic force per unit length, $\boldsymbol{V}_\infty$ the free stream speed and $\boldsymbol{\Gamma}$ the vortex circulation.
Reformulating the boundary condition (Eq. 8) in terms of the normal velocity components induced by the vortex distribution and the free-stream speed yields the linear equation as in Eq. 9,

$$\nabla \Phi_b \cdot \boldsymbol{n} = \nabla \Phi_\infty \cdot \boldsymbol{n} \quad \rightarrow \quad \boldsymbol{A\Gamma} = \nabla V_\infty \cdot \boldsymbol{n} \qquad (9)$$

where $\boldsymbol{A}$ is the aerodynamic influence matrix, in which any element (*i,j*) represents the velocity induced in *i* by a unit vortex in *j*. In principle, for each given rigid configuration the influence matrix needs to be computed just once, and then can be used to solve the problem for any desired flow condition, specified by the right-hand side of Eq. 9. In the present case, though, the solution was searched for the trimmed aircraft, which requires that the geometry adapts to each flight condition in order to keep a balanced load distribution. Therefore, the geometry being a function of the loads, the problem becomes nonlinear, and an iterative algorithm was set up in order to efficiently find the equilibrium configuration with a reduced number of evaluations.
The VLM solver, coded in Fortran, has been wrapped in Python using the F90wrap open source package [40] and included in the FAST aerodynamic module as a switchable option. To speed up the loops, a Python interface script allows data to be exchanged between the modules without writing and reading input and output files.
Before plugging the module, the code has been tested and validated against available data from the open literature and free software. Some relevant validation cases are reported in the following section.

3.2. Validation of the VLM solver

Some validation cases are here presented to attest the reliability of the employed solver.
First, to verify the predictions in symmetric flight conditions. the Warren-12 wing was used (Fig. 2), which is a standard Vortex-Lattice model used to check the accuracy of vortex lattice codes. Its parameters can be found in [41]. Since for the scope of this work multi-wing configurations have to be modelled, this test case was repeated with two different approaches. Initially the wing was modelled in the standard way as a single wing with a single set of parameters and a single aerodynamic influence matrix. Then, the semispan was split in two wings, each one with its own independent set of parameters. In this case also mutual influence matrices need to be computed, and then correctly assembled in a global one. The results are reported in Tab. Table 1, showing good agreement in both cases.

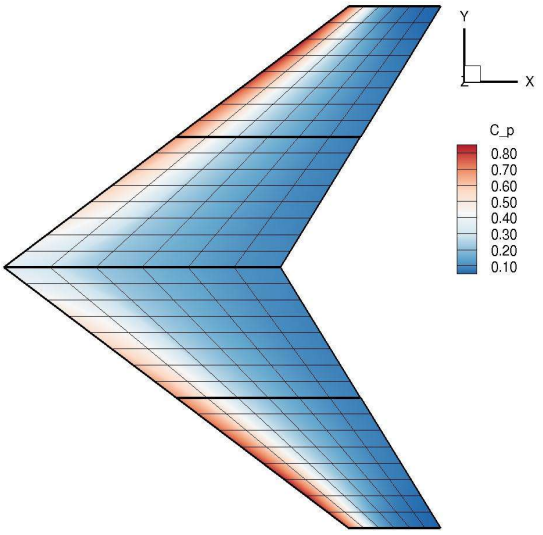

Figure 2: Warren-12 wing VLM model decomposed in four wings to validate the interaction of multi-wing configurations.

	$C_{L\alpha}$	$C_{m\alpha}$
Theory (DATCOM) [41]	2.743	-3.10
SURFACES solver [41]	2.790	-3.17
Present solver - 1w	2.780	-3.12
Present solver - 4w	2.778	-3.11

Table 1: Results for the Warren-12 wing, compared with theoretical and numerical data from [41].

Since the analyses presented in this work require the capability to predict trim configuration, a few tests were carried out to assess the accuracy of pitching moment estimation with varying geometry. To this purpose, a flat rectangular wing was analysed with sweep angles from 0° to 15°, and results were compared with those from the XFLR5 software [42] (see Fig. 3).
The last case here reported is for a multi-wing three-

dimensional configuration in asymmetric flow (Fig. 4). Again, the aerodynamic coefficients were compared with those available from XFLR5. A good matching was obtained, as shown in Tab. 2.

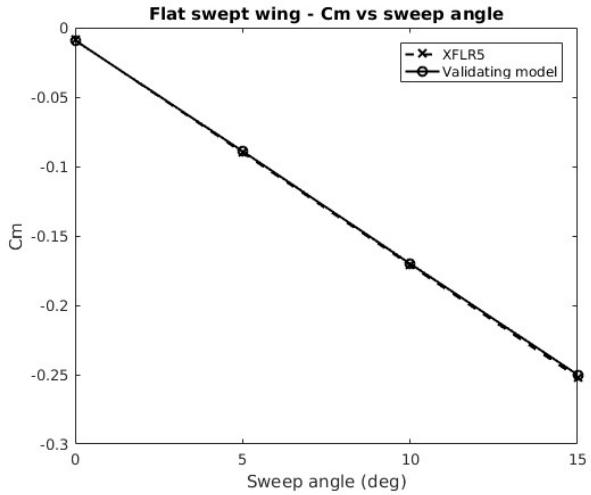

Figure 3: Pitching moment coefficient variation with increasing sweep angle, compared with results from XFLR5 [42]. Case of at flat wing of wingspan 20 m, chord 1 m, angle of attack 2°.

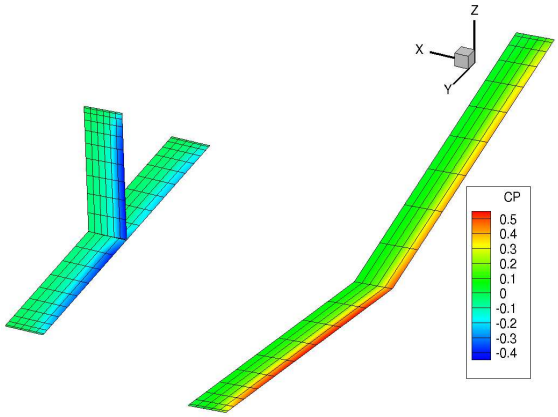

Figure 4: Multi-wing VLM configuration in asymmetric flow used for validation against the XFLR5 code[42]. Main wing: sweep angle 0°, dihedral angle = 10°. Horizontal stabilizer: span 5m, chord 1m, tilt angle 3°. Fin: span 3,5m, chord 1m. Angle of attack 2°, sideslip angle 2°.

	XFLR5 [42]	Present solver
C_L	0.123	0.131
C_D	0.001	0.001
C_m	0.384	0.377
C_l	0.007	0.006
C_n	0.009	0.009

Table 2: Aerodynamic coefficients for the validation case of Fig. 4.

4. METHODOLOGY

The first objective of the present work is to assess the robustness of the design tool when different fidelity levels are available. To this purpose, the proposed approach is to start from a reference benchmark design and use FAST to evaluate the scatter of the design outcomes when some relevant variables are perturbed. Repeating this task with each of the L0 and L1 fidelity levels (see Section 2) gives further insights on how the agreement between the two tools changes when exploring new designs.

To accomplish this, a number of design variables and their range of variation were fixed. The interest here is to compare two different aerodynamic models and investigate how their different predictions are propagated through the multidisciplinary architecture at a conceptual design level. Therefore, a few variables defining the main wing geometry are enough to accomplish the task. The selected variables are reported in Tab. 3 together with their boundaries, which were chosen in accordance with other literature on aircraft conceptual design exploration as [8].

Design variables	Ref values	Boundaries
Aspect ratio	9.48	±25%
Kink position	0.4	±15%
Sweep at 25% chord	25 [deg]	±15%
Taper ratio	0.3	±15%

Table 3: Design Variables and relative boundaries with respect to the reference CeRAS baseline.

A Design of Experiments (DOE) was carried out using a Latin Hypercube Sampling (LHS) algorithm in order to generate a population of design candidates with good projection properties [43]. This data set was used as training points to build some surrogate models as approximation of the L0-based or L1-based MDA model. For this purpose, the recent toolbox called Surrogate Model Toolbox (SMT [49]) was used. SMT is a Python package that contains a collection of surrogate modelling methods, sampling techniques, and benchmarking functions. 150 points were used to train the kriging model interpolation (Gaussian process model, [49]).

The second objective of this work is to exploit the information learned from the design exploration to perform an optimization on the reference baseline. The aim is to assess the impact of the L0 and L1 models on the optimization outcomes.

To this purpose, three different optimization algorithms were adopted. Once the kriging model is built, it can be easily used within an optimization process. A gradient free (COBYLA [44]) and a gradient based (SLSQP [46]) algorithms from the

Scipy Python library [47] were selected to be used in this study. A multi-start approach was adopted to avoid convergence to local minima. A number of 10 starting points, selected with the LHS method of [43], was found adequate. Although the mentioned algorithms were found satisfactory for the present case, further studies with involving more complex, high dimensional searches, which are envisioned for future work, would require improved techniques such as the Efficient Global Optimization (EGO [45]) algorithm available within the SMT package.
Further details on the adopted test case are given in Section 5. Results are reported and discussed in Section 6.

5. TEST CASE

The test case is for a small-medium range aircraft reproducing the features of the Airbus A320 family from available public data, mainly from the CeRAS archive [27] with some corrections and additional assumptions as in [31]. The baseline model planform is shown in Fig. Figure 5, whereas the main parameters are reported in Tab Table 4: CeRAS baseline parameters, from [31]..
The VLM representation of its configuration is also reported (Fig. 6). The former shows that the semispan of the main wing was modelled by assembling three different wings, attached together and discretized in a parametrical way such that the connections remains consistent for any global geometrical variation. Also, the number of span-wise panels was parameterized as a function of the chord-wise panels so that the two dimensions of each cell are approximately equal. The number of chord-wise panels was fixed to N = 15 after a convergence study, reported in Fig. 7. The VLM representations includes also the meanline camber of the baseline airfoil, which remains unchanged for any design change. This is visible in Fig. 8, which shows the pressure distribution during one step of the polar calculation. The drag polars of the full trimmed vehicle at cruise conditions calculated with both the L1 and the L0 aerodynamic models are plotted in Fig. 9, against some reference data from the CeRAS database. It is worth noting that the L1 model, thanks to the viscous correction of Section 3, is capable to capture the drag at low lift coefficient, which would not be possible for a pure VLM solver.

Top Level Aircraft Requirements		
Number of passengers		150
Passenger weight	[lbs]	200
Design Range	[NM]	2750
Operational Range	[NM]	800
Cruise Mach number		0.78
Approach speed	[kts]	132
Wing Geometry		
Aspect ratio		9.48
Wing break		0.4
Sweep angle at 25%	[deg]	25
Taper ratio		0.3
Propulsion		
Max thrust at sea level	[N]	117880

Table 4: CeRAS baseline parameters, from [31].

Figure 5: CeRAS baseline planform, from [31].

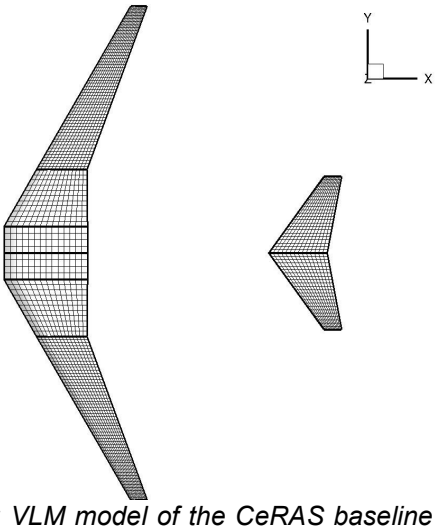

Figure 6: VLM model of the CeRAS baseline - top view.

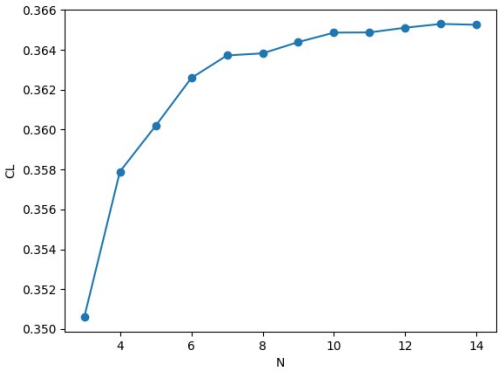

Figure 7: Convergence of the trimmed-aircraft lift coefficient with increasing number of chord-wise panels N, conducted at cruise speed, and an imposed angle of attack of 3°.

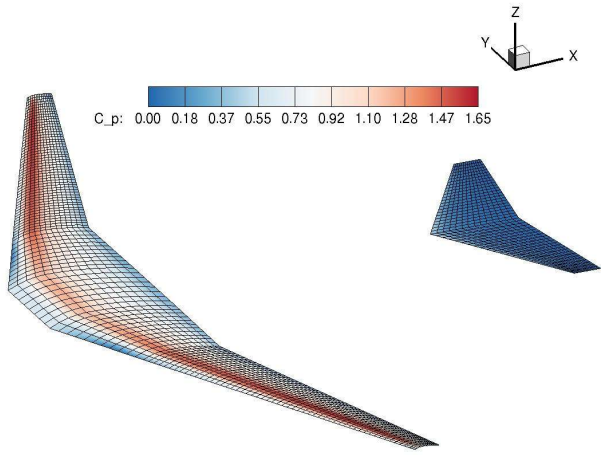

Figure 8: Pressure distribution over the trimmed CeRAS VLM model for polar computation at cruise speed.

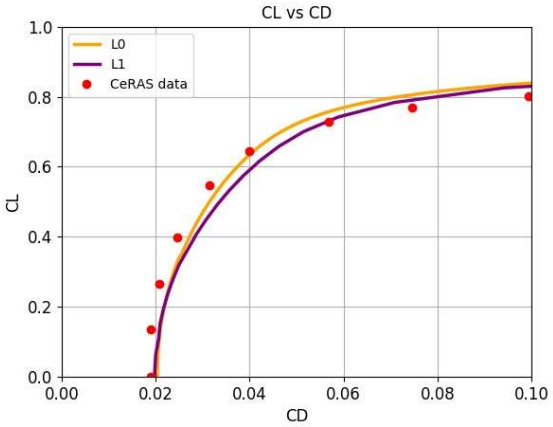

Figure 9: Cruise polars computed with the two aerodynamic models. CeRAS data are reported for comparison.

6. RESULTS

The MDA results obtained from the DOE are shown in Fig. 10 for the L0-based case, and in Fig. 11 for the L1-based case. In both cases the resulting mission fuel weight is plotted against the four design variables, and its value being proportional to the size of the spheres. It is found that the L1 aerodynamic model provides worse performance predictions compared to L0. It is not unexpected that, in both cases, the best candidates in terms of fuel weight correspond in most cases to medium-high aspect ratios. This is due to the reduction of induced drag, and is in line with the current trend towards higher aspect ratio configurations (see Fig. 1 and [6]).

A less predictable outcome, given the apparently minor differences visible in the polar predictions of Fig. 9, is the significant mismatch of fuel weight estimations over most of the examined domain.

This phenomenon is clearly reproduced in Fig. 12, where the Probability Distribution Functions (PDF) of four performance indices are extracted from the analysed data. It is found that, in three of the four cases, the L0 and L1 distributions are shifted by 3÷10%. Since the L0 model is knowledge-based and created for configurations close to the adopted baseline, its results are more clustered in the neighbourhood of the CeRAS data. Nevertheless, its reliability for innovative configurations remains questionable.

Fig. 13 shows that for design candidates featuring more significant variations from the baseline, the shift between the L0 and L1 predictions remains. Also, it can be noted that the amplitude of the scatter obtained by increasing the deviation from the baseline parameters increases in the same way for both L0 and L1. No convergence of the results from the two models is found.

The outcomes of the optimization task, where the aim is to minimize the mission fuel weight, follow the same trend, with L0 predicting a more performing minimum (see Tab. 5). It is interesting to note that the two optimal designs are appreciably different between them, as well as with respect to the baseline configuration. The task therefore turns out not to be robust enough, since considerably different optimal values are estimated, corresponding to considerably different design points.

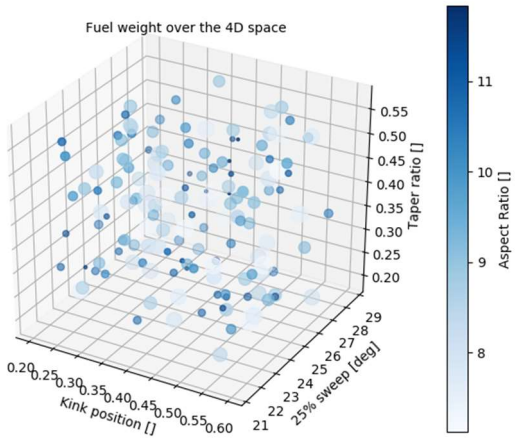

Figure 10: 5D visualization of fuel weight predictions. The size of the spheres is proportional to the normalized fuel weight. Results obtained with L0 aerodynamic model.

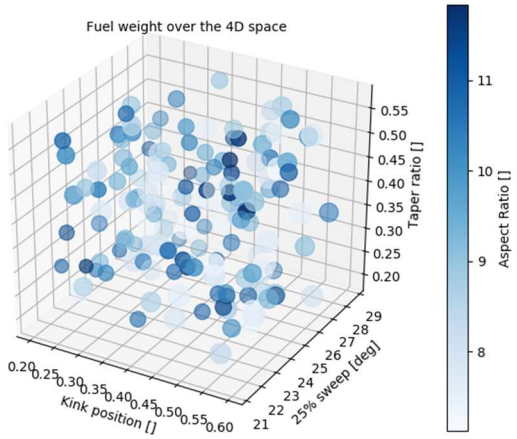

Figure 11: 5D visualization of fuel weight predictions. The size of the spheres is proportional to the normalized fuel weight. Results obtained with L1 aerodynamic model.

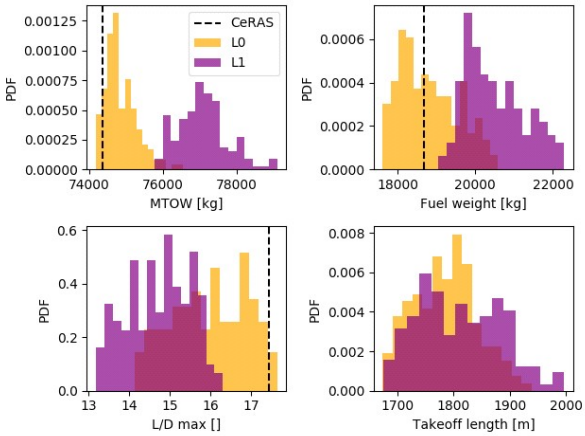

Figure 12: Probability Distribution Functions (PDF) of four performance indices, obtained with L0 and L1 for the same population of candidates. CeRAS data, when available, are reported for comparison.

7. CONCLUSIONS

A Multidisciplinary Design Analysis and Optimization framework is as computationally efficient and accurate as the least efficient and accurate method adopted for each discipline-specific analysis. Therefore, the choice of an appropriate model and an appreciation of the underlying assumptions is critical to define the intrinsic limitations of the framework. This work leverages on a sizing tool for conceptual design, named FAST, originally developed to investigate conventional concepts. FAST has been extended to include two levels of aerodynamic models: to the original one (L0), based on empirical methods created around the Airbus A320 family of aircraft, a steady/unsteady panel method was added (L1) based on the vortex lattice approach. FAST was employed to explore a design space around a reference baseline using both the L0 and L1 models. The impact of four main wing design parameters on four key figures of merit was studied for a set of 150 candidates. The Design of Experiments was performed with a Latin Hypercube Sampling algorithm, and the scatter of the results over the four-dimensional space revealed appreciable differences in the predictions obtained with the two fidelity levels.

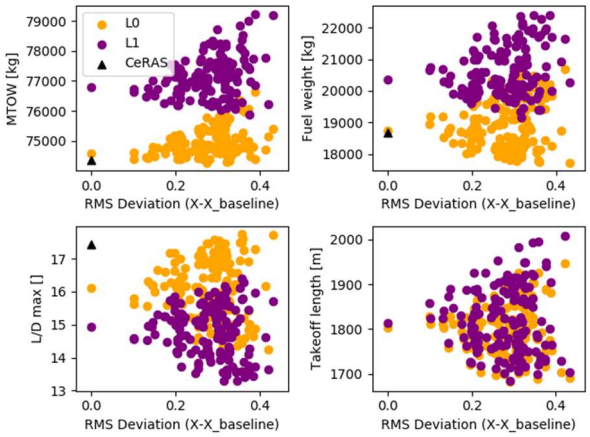

Figure 13: Scatter plot of four performance indices against the root mean square deviation of the design variables from the baseline parameters. CeRAS data are reported when available.

		AR	*wb*	*s25*	*tr*	f_{surr}	f_{true}
L0	**SLSQP**	11.76	0.57	22.1	0.51	17,654	17,731
	COBYLA	12.58	0.47	24.4	0.61	17,628	**17,574**
L1	**SLSQP**	11.24	0.30	28.7	0.36	19,041	**19,248**
	COBYLA	11.27	0.30	28.2	0.36	19,042	19,280
CeRAS baseline		9.48	0.40	25.0	0.38	-	18,678

Table 5: Fuel weight optimization results with two different optimization algorithms for the L0 and L1 data sets. f_{surr} is the optimal prediction from the surrogate model, whereas f_{true} is the value computed by FAST. The best values are highlighted in bold. The CeRAS baseline data are reported for comparison.

The following step was to assess the impact of the two aerodynamic models on the optimization of the fuel weight. To this purpose, the gathered data were fed to a kriging algorithm to generate a surrogate model of the desired performance over the design space. One gradient-based and one gradient-free

optimization algorithms were compared. After optimization, it was found that: 1) the predicted optimal fuel weight shows significant variations - around 10 t for airplanes with MTOW between 75.5 t and 76.5 t; 2) the best configurations corresponding to minimum fuel weight are also different in terms of all wing planform design parameters apart from the AR (see Fig. 14). The study provides a lucid example that small changes within the optimization chain may have a large impact on the results, calling for an approach that is robust to deal with these changes.
Moreover, both cases show that the trend for reduced fuel consumption is towards high aspect ratio configurations. This indicates that in order to provide realistic predictions aeroelastic modules need to be included within the MDAO architecture. The outcomes of this study pave the way for further improvements towards effective robust analysis capabilities for new generation aircraft concepts.

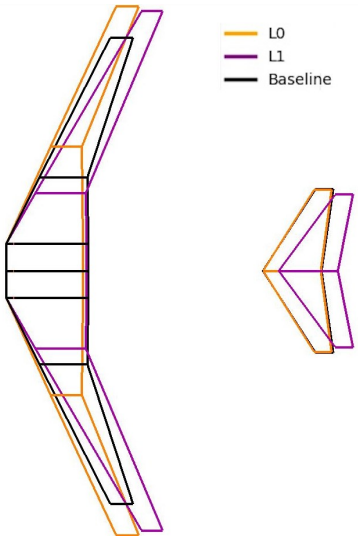

Figure 14: Optimal configurations for minimum fuel weight obtained with L0 and L1, compared to the baseline configuration.

8. REFERENCES

1. N. Cumpsty, D. Mavris, M. Kirby, Aviation and the environment: Outlook, ICAO environmental report 2019, Chapter 1. https://www.icao.int/environmental-protection/Pages/environment-publications.aspx.

2. Y.Cai, I. Chakraborty, D. N. Mavris, Integrated assessment of vehicle-level performance of novel aircraft concepts and subsystem architectures in early design, AIAA Aerospace Sciences Meeting, SciTech forum, Kissimmee, Florida, 8-12 January 2018 (AIAA Paper 2018-1741). doi:https://doi.org/10.2514/6.2018-1741.

3. M. V. Bendarkar, A. Behere, S. I. Briceno, D. N. Mavris, A Bayesian Safety Assessment Methodology for Novel Aircraft Architectures and Technologies Using Continuous FHA. AIAA Aviation Forum, 17-21 June 2019, Dallas, Texas (AIAA Paper 2019-3123). https://doi.org/10.2514/6.2019-3123.

4. Sgueglia, A., Schmollgruber, P. Bartoli, N., Atinault, O., Bénard, E. & Morlier, J. (2018). Exploration and Sizing of a Large Passenger Aircraft with Distributed Electric Ducted Fans. *AIAA Scitech Forum*, 8-12 January 2018, Kissimmee, United States (AIAA Paper 2018-1745). https://doi.org/10.2514/6.2018-1745.

5. A. Sgueglia, P. Schmollgruber, E. Bénard, N. Bartoli, J. Morlier, Preliminary sizing of a medium range blended wing-body using a multidisciplinary design analysis approach, MATEC Web of Conferences 233 (2018) 1–9. doi:10.1051/matecconf/201823300014. https://oatao.univ-toulouse.fr/21202/

6. G. Potter, Conceptual design of a strut-braced wing configuration, UTIAS National Colloquium on Sustainable Aviation, June 21-23, 2017.

7. F. Bocola, V. Muscarello, G. Quaranta, P. Masarati, Pilot in the loop aeroservoelastic simulation in support to the conceptual design of a fly by wire airplane, AIAA Atmospheric Flight Mechanics Conference, 22-26 June, Dallas,TX (AIAA Paper 2015-2557). doi:10.2514/6.2015-2557.

8. V. Trifari, M. Ruocco, V. Cusati, F. Nicolosi, A. De Marco, Multi-disciplinary analysis and optimization java tool for aircraft design, 2018.

9. Airworthiness Directives; The Boeing Company Airplanes. US Federal Aviation Administration, 14 CFR Part 39, Federal Register **136**(80), Rules and Regulations, 16 July 2015 4 pp 2012-42014.

10. L. Wang, C. Xiong, J. Hu, X. Wang, Z. Qiu, Sequential multidisciplinary design optimization and reliability analysis under interval uncertainty, *Aerospace Science and Technology,* 80 (2018), pp. 508–519. doi:10.1016/j.ast.2018.07.029.

11. J. Katz, A. Plotkin, Low-Speed Aerodynamics, Second Edition, Cambridge University Press, 2001.

12. Report of the Air Travel – Greener by Design Mitigating the environmental impact of aviation: Opportunities and priorities. (2005). *The Aeronautical Journal (1968), 109*(1099), 361-416. doi:10.1017/S0001924000000841.

13. Piperni, P., DeBlois, A. & Henderson, R. (2013). Development of a multilevel multidisciplinary-optimization capability for an industrial environment. AIAA Journal 51, 2335–2352 doi: 10.2514/1.J052180.

14. A. Sieradzki, A. Dziubinski, C. Galinski. (2016). Performance comparison of the optimized inverted joined wing airplane concept and classical configuration airplanes. Arch. Mech. Eng. **63** (3), pp. 455-470. http://dx.doi.org/10.1515/ meceng-2016-0026.

15. T. Goetzendorf-Grabowski,(2017). Multi-disciplinary optimization in aeronautical engineering. *Proceedings of the Institution of Mechanical Engineers, Part G: Journal of Aerospace Engineering*, *231*(12), 2305–2313. https://doi.org/10.1177/0954410017706994

16. T. Goetzendorf-Grabowski, J. Mieloszyk,(2017). Common computational model for coupling panel method with finite element method. Aircraft Engineering and Aerospace Technology: An International Journal **89**(5), pp. 654–662. doi: 10.1108/AEAT-01-2017-0044.

17. Kharlamov, D., Drofelnik, J., Da Ronch, A. & Walker, S. (2018). Rapid Load Calculations Using an Efficient Unsteady Aerodynamic Solver. AIAA AVIATION Forum, 25–29 June 2018, Atlanta, Georgia, USA. Doi:10.2514/6.2018-3621.

18. O. Ş. Gabor, A. Koreanschi, R. M. Botez, (2016). A new non-linear vortex lattice method: applications to wing aerodynamic optimizations. *Chinese Journal of Aeronautics*, Volume 29, Issue 5, pp. 1178-1195, ISSN 1000-9361. https://doi.org/10.1016/j.cja.2016.08.001.

19. Paul, R. C., Gopalarathnam, A. (2014). Iteration schemes for rapid post-stall aerodynamic prediction of wings using a decambering approach. *International Journal for Numerical Methods in Fluids*, Wiley Online Library (wileyonlinelibrary.com). Doi: 10.1002/fld.3931

20. Da Ronch, A., Ghoreyshi, M. & Badcock, K. J. (2011). On the generation of flight dynamics aerodynamic tables by computational fluid dynamics. *Progress in Aerospace Sciences*, 47, pp. 597-620. doi:10.1016/j.paerosci.2011.09.001

21. Choi, S., Alonso, J. J. & Kroo, H. M .(2009). Two-level multifidelity design optimization studies for supersonic jets. Journal of Aircraft **3**(46), pp. 776-790. DOI: 10.2514/1.34362

22. Afonso F., Vale, J., Lau F. & Suleman A. (2017). Performance based multidisciplinary design optimization of morphing aircraft. *Aerospace Science and Technology*, Volume 67, pp 1-12,ISSN 1270-9638. https://doi.org/10.1016/j.ast.2017.03.029.

23. Smith M. S., Sandwich, C.& NR Alley N. R. (2018). Aerodynamic analyses in support of the spanwise adaptive wing project. AIAA Aviation 2018, June 25-29, Atlanta, GA.

24. Wilson, T., Castrichini, A., Azabal1,A., Cooper2, J.E., Ajaj, R. & Herring1 M. (2017). Aeroelastic behaviour of hinged wing tips. International Forum on Aeroelasticity and Structural Dynamics (IFASD Paper 2017-216), 25-28 June, Como, Italy.

25. Toal, D. J.J. (2014). On the potential of a multi-fidelity G-POD based approach for optimization & uncertainty quantification. ASME Turbo Expo 2014: Turbine Technical Conference and Exposition, Germany.

26. Rogers, H., Lee, D., Raper, D., Foster, P., Wilson, C., & Newton, P. (2002). The impacts of aviation on the atmosphere. *The Aeronautical Journal (1968), 106*(1064), pp. 521-546. doi:10.1017/S0001924000018157.

27. CeRAS - Central Reference Aircraft Data System, [on line database] URL: https://ceras.ilr.rwth-aachen.de

28. E. Roux (2005). Pour un Approche Analytique de la Dinamique du Vol, *PhD Thesis*, ISAE-SUPAERO, Toulouse.

29. B. Nagel et al. (2014),, “Communication in Aircraft Design: Can We Establish a Common Language? ”, *28th Congress of the International Council of the Aeronautical Sciences*.

30. Schmollgruber P., Bedouet J., Sgueglia A., Defoort S., Lafage R., Bartoli N., Gourinat Y. & Benard E. (2017). Use of a Certification Constraints Module for Aircraft Design Activities. 17th AIAA Aviation Technology, Integration, and Operations Conference, 5-9 June, Denver, Colorado.

31. Schmollgruber P. (2018). Enhancement of the conceptual aircraft design process through certification constraints management and full mission simulations. *PhD Thesis.* Université fédérale Toulouse Midi-Pyrénées, Toulouse, France.

32. Dupont W. P., Colongo C. (2012). Preliminary design of commercial transport aircraft. ISAESupaero, Toulouse, France.

33. R. J. Monaghan (1953). A review and assessment of various formulae for turbulent skin friction in compressible flow. Aeronautical Research Council Tech. Rep., C.P. **142**

(15.464).

34. C. de Nicola (2015). Appunti per un corso di aerodinamica degli aeromobili. 1st ed. Class notes, Università degli Studi di Napoli "Federico II". http://wpage.unina.it/denicola/AdA/DOWNLOAD/Appunti_AdA_2014_2015.pdf.

35. J. D. Anderson Jr. (2011). Fundamentals of aerodynamics. 5th ed. McGraw-Hill.

36. M. Niţă and D. Scholz (2012). Estimating the Oswald factor from basic aircraft geometrical parameters. In: Deutscher Lift- und Raumfahrtkongress 2012, Document ID: 281424.

37. I. H. Abbott and A. E. von Doenhoff (1959). Theory of wing sections, including a summary of airfoil data. Dover publications Inc.

38. Sgueglia, A. (2019). Sizing and optimization priorities applied to a Blended Wing-Body with distributed electric ducted fans. *PhD Thesis.* Université fédérale Toulouse Midi-Pyrénées, Toulouse, France.

39. J. Katz, A. Plotkin. (2001). Low-Speed Aerodynamics, Second Edition, Cambridge University Press.

40. F90wrap: Fortran to Python interface generator with derived type support. https://github.com/jameskermode/f90wrap.

41. Surfaces-vortex lattice module, user manual. (2009). *Great OWL Publishing Engineering Software*.

42. XFLR software, http://www.xflr5.tech/xflr5.htm.

43. Jin, R. and Chen, W. and Sudjianto, A. (2005), "An efficient algorithm for constructing optimal design of computer experiments." Journal of Statistical Planning and Inference, 134:268-287.

44. Powell, M. J. (1994). A direct search optimization method that models the objective and constraint functions by linear interpolation. In *Advances in optimization and numerical analysis* (pp. 51-67). Springer, Dordrecht.

45. Jones,D. R. Schonlau, M, Welch, W.J. (1998) Efficient global optimization of expensive black-box functions, J. Glob. Optim. 13(4) 455–492.

46. Kraft, D et al. (1988). A Software Package for Sequential Quadratic Programming, DFVLR Obersfaffeuhofen, Germany.

47. E. Jones, T. Oliphant, P. Peterson, et al. (2001). SciPy: open source scientific tools for Python, http://www.scipy.org/.

48. M.A. Bouhlel, J.T. Hwang, N. Bartoli, R. Lafage, J. Morlier, J.R.R.A. Martins (2019). A Python surrogate modeling framework with derivatives, Adv. Eng. Softw., https://doi.org/10.1016/j.advengsoft.2019.03.005.

49. Williams, C. K., & Rasmussen, C. E. (2006). Gaussian processes for machine learning (Vol. 2, No. 3, p. 4). Cambridge, MA: MIT press.